Energy Proceedings
Vol 49, 2024
ISSN 2004-2965

Parametric Study of Soot Particle Deposition and Heat Transfer Properties of Exhaust Heat Exchange Tube Bundles

Yuanxun Ding[1], Hua Tian[1]*, Gequn Shu[1,2], Hongfei Zhang[3], Ping Yuan[1], Jiabao Chen[1]
1 State Key Laboratory of Engines, Tianjin University, Tianjin 300072, China
2 Department of Thermal Science and Energy Engineering, University of Science and Technology of China, Hefei 230027, China
3 School of Advanced Manufacturing Engineering, Hefei University, Hefei 230601, China
(*Corresponding Author: thtju@tju.edu.cn)

ABSTRACT

Exhaust heat exchangers play a crucial role in the waste heat recovery from internal combustion engines, yet their performance is often compromised by soot particle deposition. In this paper, a new particle deposition prediction model based on the Lagrange method is proposed, which considers thermophoresis force, drag force, and wall shear removal. Based on this model, how different tube bundle arrangements and tube geometries affect soot deposition and the thermal hydraulic performance of heat exchanger tube bundles were studied. Results indicate that increasing the transverse spacing between tubes reduces the soot deposition while increasing the longitudinal spacing has the opposite effect. Additionally, increasing the ellipticity of the heat exchange tubes lowers the fouling thermal resistance but at the cost of reduced heat transfer efficiency. We identified that a staggered tube bundle with a tube ellipticity of 0.8 and a transverse spacing of 16mm provides optimal performance without sacrificing heat transfer capacity.

Keywords: Exhaust heat exchanger, Soot particle deposition, Prediction model, Tube bundle arrangement, Thermal hydraulic performance

NONMENCLATURE

Abbreviations	
DPM	Discrete Phase Model
EGR	Exhaust Gas Recirculation
WHR	Waste Heat Recovery
Symbols	
a	Elliptical tube long axis length
b	Elliptical tube short axis length
D	Tube diameter
H_1	Transverse tube spacing
H_2	Longitudinal tube spacing

1. INTRODUCTION

The thermodynamic cycle technology is the dominant technology among the many internal combustion engine waste heat recovery (WHR) technologies that have received increasing attention [1-3]. The exhaust heat exchanger is a critical component of the thermodynamic cycle system. The complex composition of particulate matter in diesel engine exhaust leads to a large amount of particulate fouling on the heat transfer surface of the heat exchanger, leading to significant degradation of the heat exchanger's performance. Experiments [4] have shown that the deposition of diesel exhaust particulate matter in the heat exchanger leads to an increase of thermal resistance by 100% after 3h and 150% after 12h. Therefore, to reduce soot deposition and maintain the performance of the heat exchanger, the investigation and optimization of the heat exchanger structure are of great significance.

To solve the problem of particle deposition in heat exchangers, many scholars have carried out related investigations, and Kern and Seaton have divided the formation of the deposition layer into two processes: deposition and removal [5]. Wang et al. [6] have applied deposition models based on the collision of particles with wall surfaces to different types of tube-bundle heat exchangers and investigated their heat transfer and deposition characteristics, and the numerical simulation results are in good agreement with the experimental results. Han et al. [7] developed a discrete particle model (DPM) and investigated the effects of six parameters (particle diameter, flow velocity, transverse tube spacing, longitudinal tube spacing, tube geometry, and arrangement) on the fouling rate as well as heat transfer and hydrodynamic performances. Tang et al. [8] proposed a new type of tube bundle arrangement

This is a paper for the 16th International Conference on Applied Energy (ICAE2024), Sep. 1-5, 2024, Niigata, Japan.

scheme, and simulated and investigated the dynamic deposition behavior of the ash particles in the combustion process of the Zhundong coal. The current investigation of particle deposition in heat exchangers is mainly focused on micron-sized fly ash particles. While the particle size of engine exhaust particulate matter is in the submicron level (20-200 nm), which is quite distinct from micron-level fly ash particles in terms of particle force and particle motion behavior.

Investigations on the deposition of submicron engine exhaust particles in heat exchangers have been mainly based on experimental studies. Aiello et al. [9] investigated the effect of soot deposition in diesel engine exhaust on the WHR heat exchanger, and the results showed that the thermal resistance of the deposited layer in the steady state was about 70% of the total thermal resistance, and the pressure drop was about 3.25 times of the initial pressure drop. Paz et al. [10] established an exhaust soot deposition test system and experimentally investigated the variation of total particle deposition in ribbed plate heat exchangers under different operating conditions. Malayeri et al. [11] investigated the effect of cooling water temperature on deposition in an EGR heat exchanger and showed that a decrease in coolant temperature from 90°C to 25°C resulted in a 60% decrease in the thermal resistance of the deposited layer. Investigations on the deposition of engine exhaust submicron particles in heat exchangers have mainly focused on the deposition mechanism. Investigations on the optimization of heat exchanger structures aiming at inhibiting particle deposition are still relatively few.

In this paper, with the aim of reducing soot particle deposition in heat exchangers, a particle deposition model is proposed, which considers thermophoretic force, drag force, and wall shear removal. Based on this model, the effect of tube spacing and geometry on soot deposition and thermal hydraulic performance is investigated. Finally, a heat exchanger bundle arrangement scheme with improved performance was obtained through bundle structure optimization.

2. MODEL AND METHOD

2.1 Particle deposition model

According to the model of Kern and Seaton [5], the formation of the soot layer is a balance of the two processes of deposition and removal, as shown in Fig. 1.

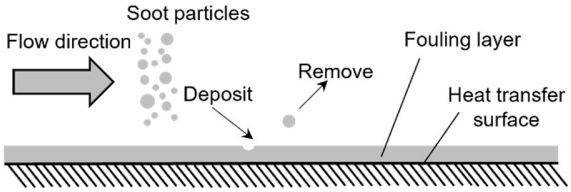

Fig. 1 Schematic diagram of particle deposition on heat transfer surface.

Thermophoresis force as the primary deposition mechanism for soot particles under internal combustion engine exhaust conditions [12, 13]. Additionally, the drag force exerted by fluid on particles, specifically turbulence, is also considered. Following Newton's second law, the equation of motion for soot particles is derived.

$$m_{\mathrm{p}} \frac{\mathrm{d}v_{\mathrm{p}}}{\mathrm{d}t} = F_{\mathrm{d}} + F_{\mathrm{T}} \tag{1}$$

Where m_{p} is particle mass, kg; v_{p} is particle motion velocity, m/s; F_{d} is the drag force on the particle, N; F_{T} is the thermophoresis force of particles, N. The drag force[14] is defined as:

$$F_{\mathrm{d}} = 1/8\pi C_{\mathrm{D}} {d_{\mathrm{p}}}^2 \rho_{\mathrm{f}} \left|v_{\mathrm{f}} - v_{\mathrm{p}}\right| (v_{\mathrm{f}} - v_{\mathrm{p}}) \tag{2}$$

Where C_{D} is drag coefficient, d_{p} is particle diameter, m; ρ_{f} is the fluid density, kg/m^3; v_{f} is velocity, m/s; Thermophoresis force[13] can be expressed as:

$$F_{\mathrm{T}} = -D_{\mathrm{T}} \frac{1}{m_{\mathrm{p}} T} \vec{\nabla} T \tag{3}$$

Where D_{T} is the thermophoresis coefficient.

Based on elastic-plastic deformation and energy dissipation during particle-wall collisions, the post-collision state of the particle is determined according to rebound energy criteria. The collision process of particles on the surface of the heat exchange tube at the incident velocity v_i and Angle θ is depicted in Fig. 2. The possibility of deposition is determined using energy conservation in this collision process, as described by the following equation:

$$Q_{\mathrm{k,i}} + Q_{\mathrm{A,a}} = Q_{\mathrm{el}} + Q_{\mathrm{pe}} + Q_{\mathrm{p}} \tag{4}$$

Q_k is the initial kinetic energy of particles, J; $Q_{A,a}$ is the surface adhesion energy due to the contact between the particle and the wall, J; Q_{el} and Q_{pe} are the elastic energy stored by the elastic and plastic deformation of particles, respectively. Q_p is the energy loss caused by plastic deformation, J;

$$Q_{\mathrm{el}} + Q_{\mathrm{pe}} \leqslant Q_{\mathrm{A,r}} \tag{5}$$

$$Q_{\mathrm{A,r}} = Q_{\mathrm{A,a}} + 10.4 r^4 \left(\frac{E^{*2}\Gamma^5}{F^4} \right)^{1/3} \tag{6}$$

When the elastic energy of the particles is not greater than the adhesion energy $Q_{A,r}$ the particles will be deposited on the wall, otherwise they will rebound. $Q_{A,r}$ is the adhesion energy after collision, J.

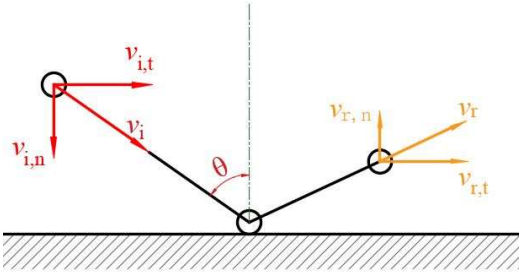

Fig. 2 Schematic diagram of particle collision with heat transfer wall.

2.2 Particle removal model

The growth of particle-deposited fouling in a heat exchanger has an asymptotic value that is controlled by both the deposition rate and the removal rate. At the initial moment, the deposition rate is large and the fouling layer grows rapidly, and as the fouling layer grows the removal rate becomes larger and approaches the deposition rate. In the present work, the removal rate of fouling is considered to be proportional to the thickness of the fouling layer, the local wall shear stress, and inversely proportional to the strength factor of the fouling layer. The removal rate function is [9]:

$$m_{\mathrm{r}} = k \left(\frac{\tau_{\mathrm{w}}}{\psi} \right) x_{\mathrm{f}} \tag{7}$$

Where m_{r} is the fouling removal rate, k is the removal constant, τ_{w} is the flow shear stress at the surface of the deposit layer, ψ is the intensity of the deposit layer, and x_{f} is the fouling thickness.

The net deposition rate is:

$$\eta = m_{\mathrm{d}} - m_{\mathrm{r}} \tag{8}$$

2.3 Computational domain and boundary conditions

The simplified computational domain of the model is shown in Fig. 3. Velocity inlet, pressure outlet, and symmetric boundary conditions are employed. In this study, the SST K-ω turbulence model [15] in FLUENT is employed to simulate gas flow. The DPM model is used to obtain the particle force, velocity, and position information in the flow field, and the deposition and removal models are loaded to the wall boundaries through the UDF function. The inlet velocity is 23.28 m/s, the inlet temperature is 747.42 K, the outlet pressure is 101.325 kPa, and the constant wall temperature is 353.15 K. The diameter of soot particles was 200 nm, and the concentration of soot particles was 3.28×10^{-8} kg/s. The structural parameters of the original tube bundle are as follows: tube diameter D = 14 mm, H_1 = 18 mm, H_2 = 15 mm.

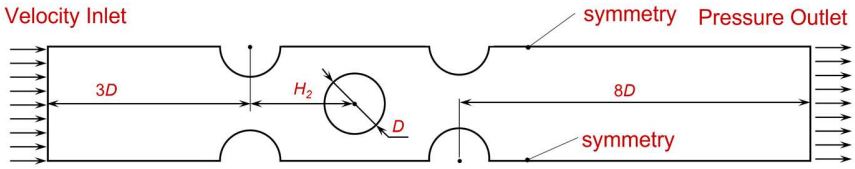

(a) Staggered arrangement of round tube

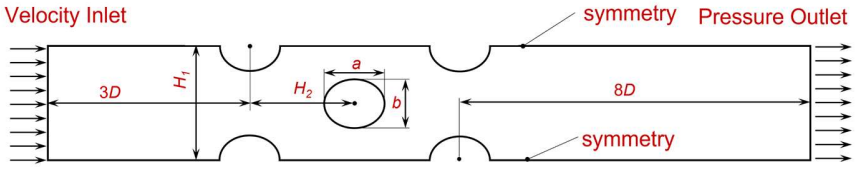

(b) Staggered arrangement of elliptical tube

Fig. 3 Schematic of the structure of tube banks.

3. MODEL VALIDATION

3.1 Grid generation and independence validation

The computational grid is generated by workbench Mesh, the non-structural grid was adopted and the grids at the tube wall were refined. For the tube bank model in this paper, the number of meshes 93761, 100069, 118582, 135666, and 145119 were used for the

calculation. When the number of grids reaches 145119, the relative change of the calculation results is less than 1% if the mesh refinement is continued. The calculation results are considered to be independent of the grid. The same method was used to generate the grids for the different structural models in this paper.

Table 1 Influence of the number of grids on the calculation results.

Number of Grids	Deposition Rate η (%)	Heat Transfer Rate Q (W)	Relative Variability of η or Q (%)
93 761	8.34	9065.21	16.43/0.45
100 069	9.98	9024.56	3.48/0.10
118 582	10.34	9015.48	5.83/0.08
135 666	10.98	9008.32	1.08/0.02
145 119	11.10	9007.01	0.18/0.05
153 240	11.08	9011.64	0.18/0.05

3.2 Model's heat transfer validation

To evaluate the accuracy of the model, a comparison was made between the model calculation results and the heat transfer correlation equation [16] results for the tube bundle heat transfer structure. As shown in Fig.4, the model calculation results had good accuracy.

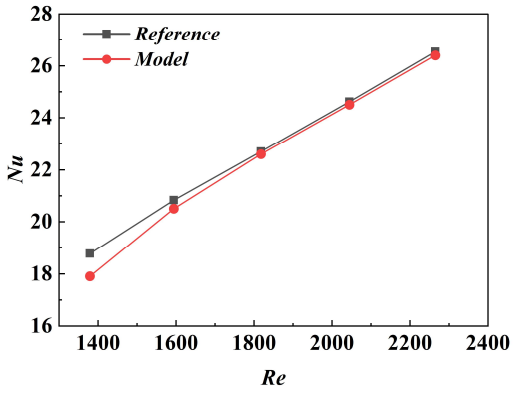

Fig. 4 Comparison of model and heat transfer correlation equation.

4. RESULTS AND DISCUSSION

4.1 Effect of tube spacing on deposition rate

The particle deposition rates in the heat exchange tube bundle with different transverse/longitudinal tube spacing arrangements were compared and analyzed, as shown in Fig. 5. With the increase of transverse tube spacing, the flow area outside the tube is increased, the collision probability between particles and tube wall is reduced, and the deposition rate is reduced. However, the increase in the longitudinal tube spacing allowed the development of a tail vortex behind the tube (as shown in Fig. 6). More soot particles are wrapped back by the airflow to hit the tube wall, thus making the deposition rate increase. The effect of transverse tube spacing on particle deposition is more obvious than that of longitudinal tube spacing.

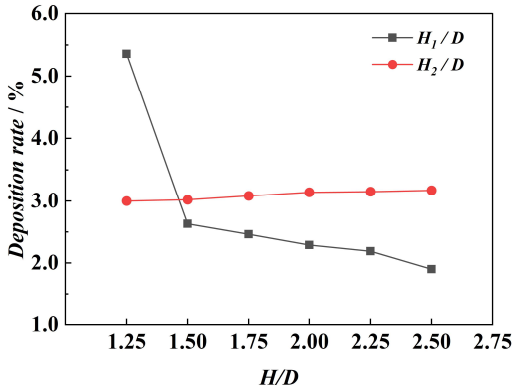

Fig. 5 Effect of transverse/longitudinal tube spacing on deposition rate.

4.2 Effect of tube ellipticity

The soot deposition can be reduced by increasing the transverse tube spacing and decreasing the longitudinal tube spacing. The elongated shape of the elliptical tube can satisfy the condition of large transverse tube spacing and small longitudinal tube spacing. In addition, the streamlined shape of the elliptical tube makes the

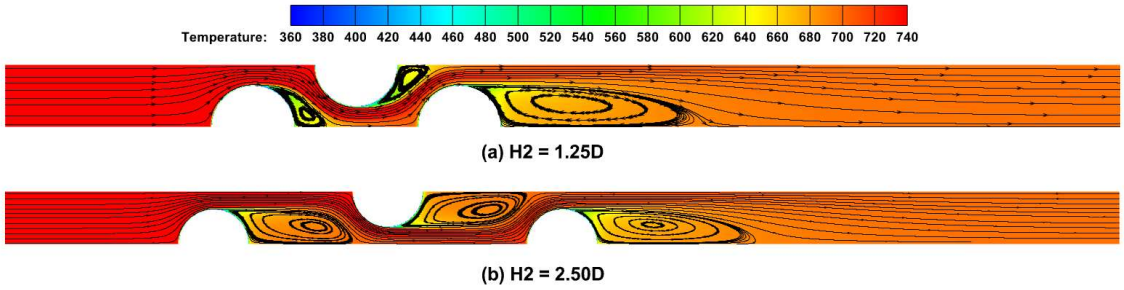

Fig. 6 Streamline diagram of tube bundle: (a) H_2=1.25D (b) H_2=2.50D.

elliptical tube have the characteristics of reducing flow resistance.

In this section, the effect of ellipticity of elliptical tubes on soot deposition and flow heat transfer is analyzed. Under the condition that the heat transfer area of the heat exchanger tube remains fixed, the selected axis-length ratio is in the range of 0.5 to 1. The ellipticity b/a is the ratio of the short axis to the long axis of the ellipse (as shown in Fig. 3). When the axis length ratio b/a = 1 is a round tube, the smaller the axis length ratio, the flatter the shape of the heat exchanger tube.

Fig. 7 shows the soot deposition and flow heat transfer performance of different ellipticity heat exchange tube bundles. With the increase of the flatness of tube, the deposition rate of soot particles decreases obviously. The deposition rate of elliptical tube bundle with b/a=0.6 decreased by 61.98% compared with round tube bundle. As a cost, the heat transfer performance of elliptical tube bundle decreased by 35.86% compared with round tube bundle.

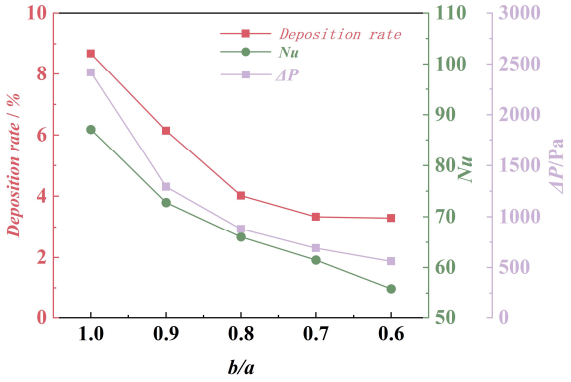

Fig. 7 Effect of tube ellipticity on deposition rate and flow heat transfer performance.

As shown in Fig. 8, due to the streamlined shape of the elliptical tube, the separation point of the boundary layer at the back of the tube is shifted back, so that the backflow region of the tube is compressed. Soot particle deposition due to the wake flow behind the tube is reduced.

4.3 Deposition distribution of different shaped tube bundles

As shown in Fig. 9, For the first column of tubes, most of the particle deposition occurs in the range of 0-90° in front of the tube, and the flatter the elliptical tube, the more concentrated the deposition. The round and large b/a elliptical tube deposition peaks are shifted back and do not reach the deposition peak at 0° in front of the tube, which is due to the existence of the flow stagnation zone in front of the tube and the good particle mobility. The amount of deposition at the back of the tube is small for the different shapes of tubes. This is due to the underdevelopment of the backflow region after the first column of tubes.

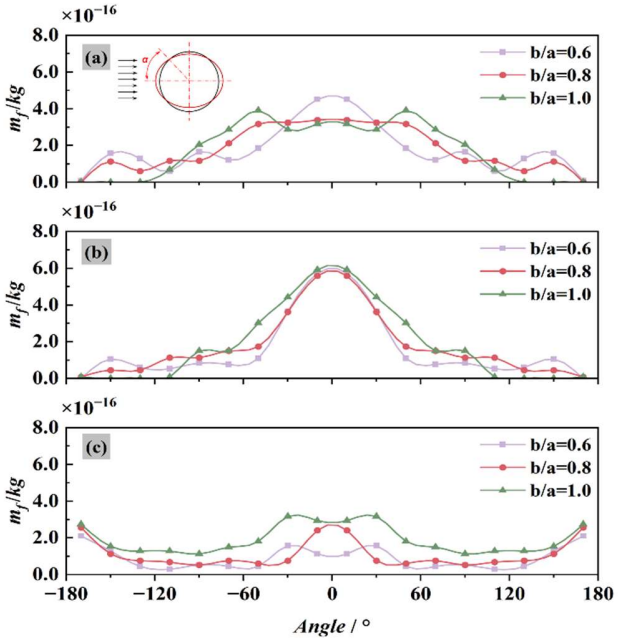

Fig. 9 Deposition distribution of different shaped tube bundles:(a) first column (b) second column (c) third column.

For the second column, the soot particle deposition is concentrated in the range of 0-60°. The angular range of particle deposition was more concentrated compared to the first row of tubes. This is due to the first column

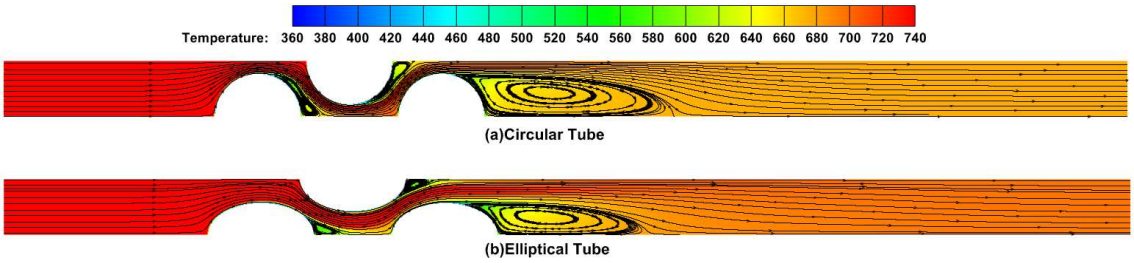

Fig. 8 Streamline diagram of tube bundle: (a) Round tube (b) Elliptical tube(b/a=0.6).

tube play the role of the particle aggregation. And the amount of deposition at the back of the second column of tubes is small, as the backflow region is compressed.

For the third column of tubes, there is significant deposition in both the front and back regions of the tubes. And the deposition on elliptical tubes is lower than that on round tubes for most of the angles.

4.4 Optimized tube bundle arrangement structure

To minimize soot particle deposition without compromising heat transfer, the tube bundle arrangement has been modified. The H_1 dimension has been reduced to 16 mm, and the b/a ratio ranges from 0.5 to 1. In comparison with a round tube bundle (H_1=18 mm), the elliptical tube bundle (H_1=16 mm) with b/a=0.8 exhibited a 1.09% increase in heat transfer, a 43.32% reduction in deposition rate, and a 28.25% decrease in pressure drop, making it a superior tube bundle structure. It should be added that the reduction of the transverse tube spacing has resulted in an increase in the number of heat exchanger tubes in the optimized structure compared to the original structure (from 26 round tubes to 29 elliptical tubes).

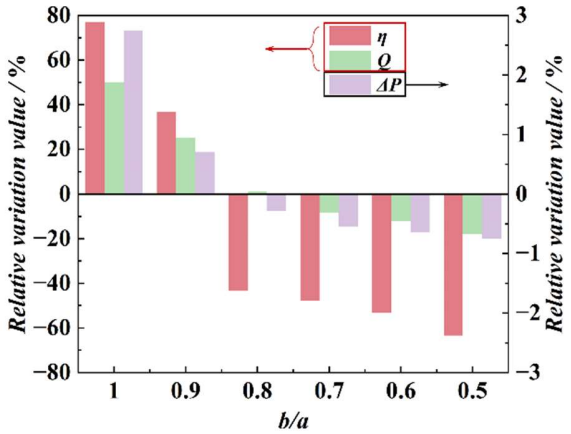

Fig. 10 Performance comparison between small transverse tube spacing elliptical tube bundle and original structure.

Table 2 Comparison between original and optimized tube bundle structure.

b/a-H_1	Deposition Rate η	Heat Transfer Rate Q	Pressure drop ΔP
1.0-18	8.68	23.37 kW	2.42 kPa
0.8-16	4.92	23.63 kW	1.73 kPa
	-43.32%	1.09%	-28.25%

5. CONCLUSIONS

In this paper, the heat exchanger for waste heat recovery of the internal combustion engine is numerically simulated. Based on the DPM model, a new particle deposition prediction model is developed, which takes into account the thermophoresis force, drag force, and wall shear removal. The effects of different tube spacing and tube geometry on soot deposition and thermal hydraulic performance of tube bundle of heat exchanger were studied. The main conclusions are described as follows:

(1) Increasing the transverse spacing between tubes can reduce the deposition of soot, but increasing the longitudinal spacing between tubes has the opposite effect.

(2) Increasing the ellipticity of the heat exchange tube (reducing b/a) can reduce the thermal resistance of the deposited layer but at the cost of reducing the heat transfer efficiency.

(3) A staggered tube bundle with an ellipticity of 0.8 and a transverse spacing of 16mm provides the best performance without sacrificing heat transfer capacity.

REFERENCE

[1] Wang J, Yan Z, Wang M, Ma S, Dai Y. Thermodynamic analysis and optimization of an (organic Rankine cycle) ORC using low grade heat source. Energy. 2013;49:356-65.

[2] Peris B, Navarro-Esbrí J, Molés F. Bottoming organic Rankine cycle configurations to increase Internal Combustion Engines power output from cooling water waste heat recovery. Applied Thermal Engineering. 2013;61:364-71.

[3] Zhang X, Wang X, Yuan P, Ling Z, Bian X, Wang J, et al. Experimental study on the comparative performance of R1233zd (E) and R123 for organic rankine cycle for engine waste heat recovery. International Journal of Green Energy. 2024:1-8.

[4] Zhang R, Charles F, Ewing D, Chang J-S, Cotton J. Effect of diesel soot deposition on the performance of exhaust gas recirculation cooling devices. SAE Technical Paper; 2004.

[5] Kern D. A theoretical analysis of thermal surface fouling. Br Chem Eng. 1959;4:258-62.

[6] Wang F-L, Tang S-Z, He Y-L, Kulacki FA, Yu Y. Heat transfer and fouling performance of finned tube heat exchangers: Experimentation via on line monitoring. Fuel. 2019;236:949-59.

[7] Han H, He Y-L, Tao W-Q, Li Y-S. A parameter study of tube bundle heat exchangers for fouling rate reduction. International journal of heat and mass transfer. 2014;72:210-21.
[8] Tang S, Ding L, Zhou J, Shen B, Li H. Dynamic CFD modeling and evaluation of ash deposition behaviors during Zhundong coal combustion. Fuel Processing Technology. 2022;234:107340.
[9] Aiello VC, Kini G, Staedter MA, Garimella S. Investigation of fouling mechanisms for diesel engine exhaust heat recovery. Applied Thermal Engineering. 2020;181:115973.
[10] Paz C, Suárez E, Concheiro M, Porteiro J. Experimental study of soot particle fouling on ribbed plates: Applicability of the critical local wall shear stress criterion. Experimental thermal and fluid science. 2013;44:364-73.
[11] Razmavar AR, Malayeri MR. Thermal performance of a rectangular exhaust gas recirculation cooler subject to hydrocarbon and water vapor condensation. International Journal of Thermal Sciences. 2019;143:1-13.
[12] Abd-Elhady M, Malayeri M. Asymptotic characteristics of particulate deposit formation in exhaust gas recirculation (EGR) coolers. Applied Thermal Engineering. 2013;60:96-104.
[13] Abarham M, Hoard J, Assanis D, Styles D, Curtis EW, Ramesh N. Review of soot deposition and removal mechanisms in EGR coolers. SAE International Journal of Fuels and Lubricants. 2010;3:690-704.
[14] Zhang Y, Zhao Y, Lu L, Ge W, Wang J, Duan C. Assessment of polydisperse drag models for the size segregation in a bubbling fluidized bed using discrete particle method. Chemical Engineering Science. 2017;160:106-12.
[15] Wang F-L, He Y-L, Tang S-Z, Kulacki FA, Tao Y-B. Multi-objective optimization of a dual-layer granular filter for hot gas clean-up by using genetic algorithm. Applied Energy. 2019;248:463-74.
[16] Zhukauskas AgAf. Heat transfer in banks of tubes in crossflow of fluid: Izd-vo" Mintis"; 1968.